

ISTITUTO NAZIONALE DI FISICA NUCLEARE  
Laboratori Nazionali di Frascati

LNF-81/78

P. Berthet, R. Frascaria, B. Tatischeff, J. Banaigs, J. Berger,  
J. Duflo, L. Goldzahl, F. Plouin, M. Boivin, F. Fabbri, P. Pi-  
cozza and L. Satta:  $p + {}^3\text{He}$  ELASTIC BACKWARD SCATTER-  
ING AT INTERMEDIATE ENERGIES

Estratto da:  
Physics Letters 106B, 465 (1981)

$p + {}^3\text{He}$  ELASTIC BACKWARD SCATTERING AT INTERMEDIATE ENERGIES

P. BERTHET, R. FRASCARIA and B. TATISCHEFF  
*IPN, Orsay, France*

J. BANAIGS, J. BERGER, J. DUFLO, L. GOLDZAHL and F. PLOUIN  
*ER 54, Saclay, France*

M. BOIVIN  
*LNS, Saclay, France*

and

F. FABBRI, P. PICOZZA and L. SATTÀ  
*INFN, Frascati, Italy*

Received 9 July 1981

The  $p\text{-}{}^3\text{He}$  elastic backward scattering cross sections have been measured in the laboratory kinetic energy range  $700 \leq T_p \leq 1700$  MeV for backscattered proton angle  $160^\circ < \theta_p < 180^\circ$  in the c.m. A change in the slope of the cross sections and a bump in the  $180^\circ$  excitation function are observed around  $T_p = 1300$  MeV. These features are explained as due to baryonic excitation in intermediate states.

Backward scattering of protons by  ${}^3\text{He}$  have been previously studied at 415, 600 and 800 MeV [1]. The main features of these data, in particular the fact that the cross sections are nearly the same at 415 and 600 MeV were interpreted in a one pion plus 2 N exchange mechanism, as due to a  $\Delta$  resonance in the intermediate state in the s-channel. The question arose immediately of whether it is possible to excite the other baryon states or eventually propagate a double  $\Delta$  in the  ${}^3\text{He}$  nucleus. Because of the new facility offered at the Saturne National Laboratory on the SPES 4 beam line we have been able to pursue the  $p\text{-}{}^3\text{He} \rightarrow {}^3\text{He} p$  measurements at kinetic energies as high as 1700 MeV proton and at proton angles very close to  $180^\circ$  by detecting the recoiling  ${}^3\text{He}$  nucleus at very forward angles.

The experimental set up [2] is summarized as follows (see fig. 1). The proton beam extracted from the

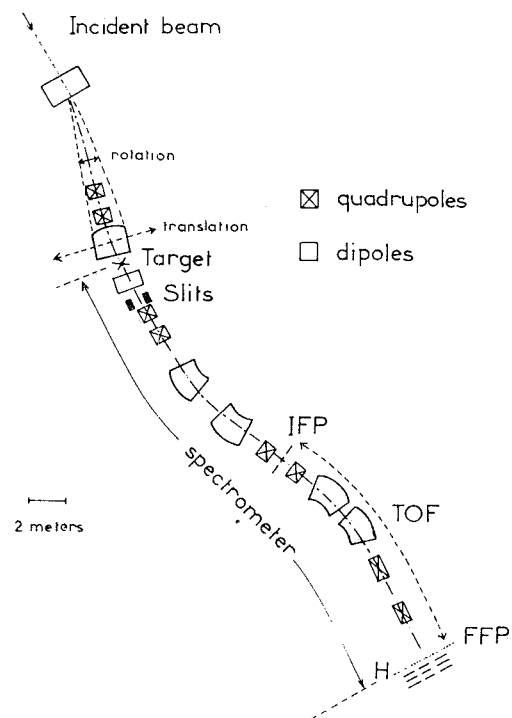


Fig. 1. Experimental layout. Legend: IFP = intermediate focal plane; TOF = time of flight basis; FFP = final focal plane; H: plastic scintillator hodoscope.

synchrotron is focussed on the target which is a liquid  ${}^3\text{He}$  target with a thickness of  $300 \text{ mg cm}^{-2}$ . The scattering angles are obtained by changing the bending of the incident proton beam, the intensity of which is kept at  $2 \times 10^{11}$  protons per burst. The recoiling  ${}^3\text{He}$  particles were detected using the SPES IV spectrometer at angles ranging from  $1^\circ_{\text{lab}}$  to  $10^\circ_{\text{lab}}$  which corresponds to proton center of mass angles from  $160^\circ$  to  $178^\circ$ . Full vertical and horizontal aperture of  $1^\circ$  were used, corresponding to an angular resolution in the center of mass of  $\Delta\theta = 2^\circ$  (full width).

The SPES IV beam mainly consists of four dipoles and six quadrupoles yielding an intermediate focal plane at 16 meter from the target and a final focal plane at 32 meter from the target. Another dipole is placed just behind the target and before the collimator slits, allowing us to discriminate between particles emerging from the target and having different momentum  $p/z$  as close as  $100 \text{ MeV}/c$ . This permits the cross section measurements at very small angles, rejecting the primary beam from the SPES IV spectrometer entrance which is tuned for the  ${}^3\text{He}$  detected particles.

Three thin plastic scintillators (0.1 mm thickness) were placed in the intermediate focal plane each covering 1.5% in momentum. In the focal plane 19 plastic scintillators defining an hodoscope detector of 0.2% momentum resolution over 3.8% momentum range were followed by three rows of 3 plastic scintillators. We set up 3 telescopes, each one of it being defined by one counter in the intermediate focal plane, 6 counters of the hodoscope plane and one counter of the three last scintillator planes, the coincident events being registered and labelled as a function of their position in the final focal plane. Due to the 16 meter time of flight distance and the three energy loss measurements on each event, a very high separation of the background is obtained: in the worst case, at 1700 MeV incident kinetic energy and at  $\theta_{3\text{He}} = 2^\circ$ , the ratio between the elastic peak and the background under the peak is about 7.

The beam current was monitored by three telescopes each made up of 3 plastic scintillators, two of them viewing a very thin  $\text{CH}_2$  film upstream and one viewing the liquid target. The calibration of these monitors are obtained at each energy by activity measurements from  ${}^{12}\text{C}(p, pn){}^{11}\text{C}$ . The variation of the stability of the monitors during the experiment and the uncertainty coming from the absolute beam cali-

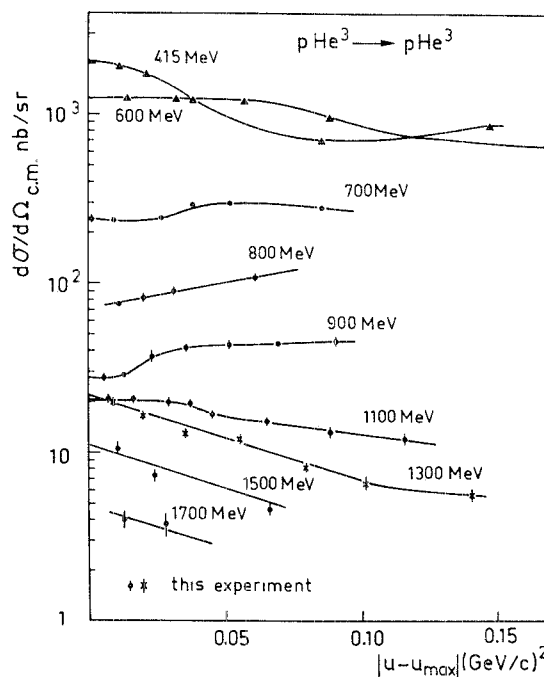


Fig. 2. Experimental results of the backward  $p\tau \rightarrow \tau p$  elastic scattering at various incident proton energies as a function of  $|u - u_{\text{max}}|$  where  $u_{\text{max}}$  is the value of  $u$  at  $\theta_p = 180^\circ$ . The experimental data at 415 and 600 MeV are from a previous experiment (ref. [1]).

bration or the target thickness lead to an absolute error of  $\pm 9\%$ .

All the experimental data are shown in fig. 2 as a function of  $|u - u_{\text{max}}| = 2p^2(1 - \cos\theta)$  for the seven different incident energies indicated on the curves to guide the eye. The error bars are only statistical so an overall uncertainty of  $\pm 9\%$  must be added. The data points at 415 and 600 MeV are from ref. [1]. Two main features appear: the change of slope between 800 MeV and 1100 MeV of the angular distribution and the constance of the absolute value of the cross section between 900 MeV and 1300 MeV for  $\theta = 180^\circ$ .

In fig. 3 is plotted the  $\theta_p = 180^\circ$  excitation function extracted from our data as a function of the laboratory kinetic energy of the incident protons showing the two large structures at 400–600 MeV and 900–1300 MeV. In the same figure is also plotted the  $\theta_\pi = 180^\circ$  excitation function at the  $pd \rightarrow t\pi$  – or isospin equivalent – reactions [3–5]; the new data between 600 and 1500 MeV (squares) were taken in the same

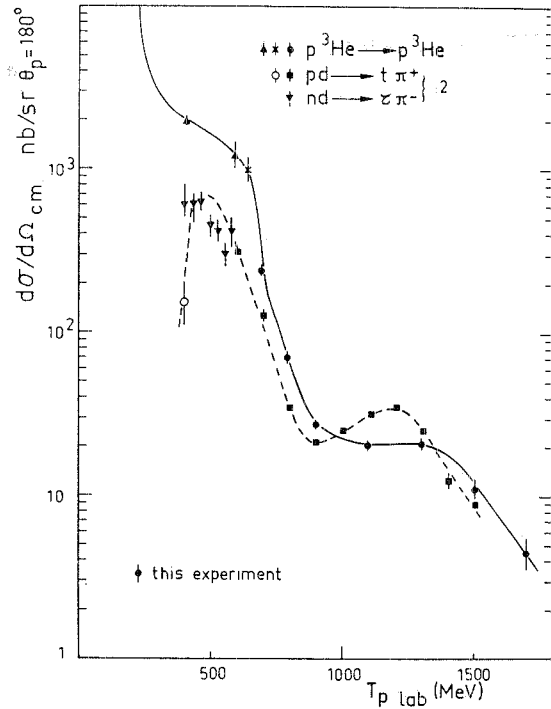


Fig. 3. The  $\theta_p = 180^\circ$  excitation functions of the  $p\tau \rightarrow \tau p$  elastic scattering extrapolated from the results of this experiment and of ref. [1] and of the  $pd \rightarrow t\pi^+$  reaction [2-5] as a function of the same laboratory kinetic energies of the incident protons. The curves are drawn to guide the eye.

run [2] using a  $608 \text{ mg/cm}^2$  liquid deuterium target. The striking similarity of the data for these two reactions can be explained, if use is made of the one pion exchange model [6] where all the  $B = 2$  exchange reactions are related to the  $\pi d \rightarrow d\pi$  backward elastic as the elementary interaction. For instance in the  $p\tau \rightarrow \tau p$  reaction, the exchanged pion carries the transferred momentum and the cross section is peaked at zero relative momentum of the deuteron in  $^3\text{He}$ , corresponding to the deuteron at rest in the lab: that is why  $p\tau \rightarrow \tau p$  and  $pd \rightarrow t\pi$  must be similar for the same lab kinetic energy.

The  $p\tau \rightarrow \tau p$  excitation function at  $\theta_p = 180^\circ$  has been calculated using the model of Barry [6] where the form factor has been slightly modified [7]:  $|\psi_\tau(0)|^2$  is replaced by  $R_{23}(0)$ , which is the overlap between a deuteron and a  $^3\text{He}$  for  $\rho = 0$ . The value of  $R_{23}(0)$ , coming out of the resolution of the 3-body bound state [8] varies between  $0.096$  and  $0.14 \text{ fm}^{-3}$

depending on the depth of the attractive part of the N-N potential used in this calculation.

The result of this calculation is shown in fig. 4 in comparison with the experimental data plotted as a function of the total c.m. energy. The agreement in shape reflects the similarity of the  $p\tau \rightarrow \tau p$  and  $pd \rightarrow t\pi$  cross sections. The absolute value seems to be not badly reproduced. However, the  $B = 2$  exchange reactions are discussed more fully below: the  $pd \rightarrow t\pi$  reaction can also be expressed in terms of the  $\pi d \rightarrow d\pi$  scattering in the one pion exchange model (OPE) [6]. The same form factor appears, so if the ratio

$$R_1 = \frac{d\sigma(pd \rightarrow t\pi)}{d\Omega} / \frac{d\sigma(p\tau \rightarrow \tau p)}{d\Omega},$$

is formed at  $\theta_\pi = \theta_p = 180^\circ$ , it should be equal to

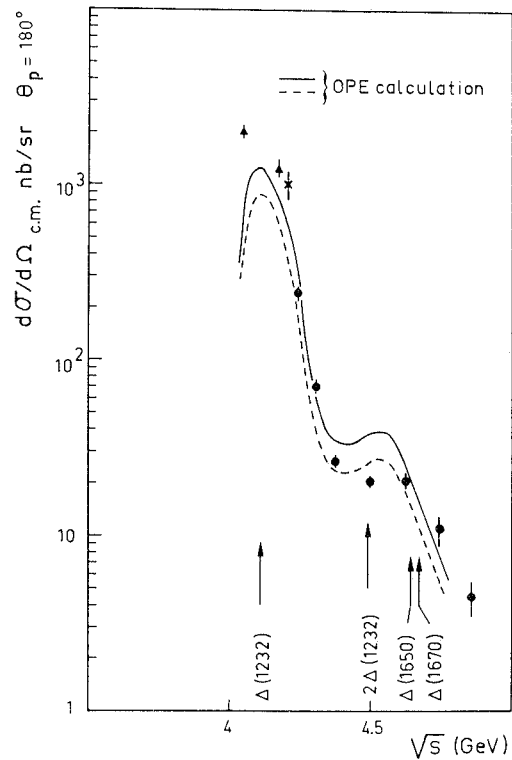


Fig. 4. The experimental  $\theta_p = 180^\circ$   $p\tau \rightarrow \tau p$  excitation function in comparison with the calculation in the OPE model as a function of the total c.m. energy of the system. The symbols  $\Delta$  and  $\times$  correspond to ref. [1] and  $\bullet$  to this experiment. The arrows indicate the intermediate exchanged mass resulting of the OPE calculation. Curves: the continuous (dashed) line corresponds to  $R_{23}(0) = 0.14 \text{ fm}^{-3}$  ( $0.096$ ).

$$R_1 = \frac{4}{3} \frac{|t_\pi|^2 S_{\pi d} S_{p t}}{|p_d|^2 (S_{\pi t})^2} R_2,$$

where

$$R_2 = \frac{d\sigma(\pi d \rightarrow d\pi)}{d\Omega} \bigg/ \frac{d\sigma(\text{pd} \rightarrow t\pi)}{d\Omega},$$

and is independent of the nuclear structure.

In the range of energies  $600 \text{ MeV} < T_p < 1200 \text{ MeV}$  the theoretical predictions of the OPE model are  $R_1 = 25 \times 10^{-3} R_2$  and  $R_1 = 8.6 \times 10^{-2} R_2$ , respectively, at  $T_p = 600$  and  $T_p = 1200 \text{ MeV}$ . If a comparison is made between the experimental data of the  $p\tau \rightarrow \tau p$ ,  $\text{pd} \rightarrow t\pi$  and  $\pi d \rightarrow d\pi$  [9] excitation functions at  $\theta_p$  or  $\theta_\pi = 180^\circ$ , the relation between  $R_1$  and  $R_2$  is  $R_1 = 10^{-3} R_2$  and  $R_1 = 2.9 \times 10^{-2} R_2$ , respectively, for  $T_p = 600$  and  $1200 \text{ MeV}$ .

So the calculation is a factor of 4 (at  $1200 \text{ MeV}$ ) to 25 (at  $600 \text{ MeV}$ ) too high when the  $p\tau \rightarrow \tau p$  excitation function is explained in terms of the  $\pi d \rightarrow d\pi$  excitation function.

This difficulty of the OPE model in giving simultaneously the correct absolute value for the two  $B = 2$  exchange reaction  $p\tau \rightarrow \tau p$  and  $\text{pd} \rightarrow t\pi$  has also been encountered in the description of the  $B = 1$  exchange reactions  $pp \rightarrow d\pi$  and  $\text{pd} \rightarrow dp$  [10]. Recently Anjos et al. [11] have suggested that the approximation of removing from the integral the pions and delta poles for the value  $q = 0$  of the relative momentum of nucleons inside the deuterons is too crude; if this approximation is made the  $\text{pd} \rightarrow dp$  cross section calculated in terms of the  $\pi N \rightarrow N\pi$  scattering is a factor 40 larger than the experimental one. When the integration is correctly done on the two internal loop variables the  $\text{pd} \rightarrow dp$  is reproduced both in shape and absolute value (with a neutron pick up term added incoherently). A similar explanation can be used for the  $B = 2$  exchange reactions: the calculated OPE coupling strength  $\zeta$  of Barry [6] in the wave function integration approximation is probably too high. Other effects can also contribute to reduce the discrepancy of this model with the data such as off-shell effects or initial- and final-state interactions as suggested by Keister and Kisslinger [12]. In their calculation of the  $pp \rightarrow d\pi^+$  forward differential cross sections in terms of  $\pi N$  scattering, these authors show that distortion effects at high energy can reduce the calculated cross section by

a factor of 2 to 3 and improve the agreement with the experimental results. Distortion effects in a calculation of the  $\text{pd} \rightarrow t\pi^+$  in terms of the  $\pi d \rightarrow d\pi$  cross sections, could produce a similar effect, increasing the theoretical ratio  $R_2$  and so reducing the discrepancy between the experimental and the theoretical ratio  $R_1$ . Nevertheless the OPE graph, if correctly calculated, remains dominant at backward angles. In the same fig. 4 are indicated the masses of the different  $\Delta$  excited in the intermediate state calculated in the OPE scheme: the first bump is clearly associated with the excitation of the  $\Delta_{33}(1232)$ . The broadening of the width is due to the Fermi momentum distribution of the nucleons in  $^3\text{He}$ .

The second structure at  $\sqrt{s} = 4.5 \text{ GeV}$  is tentatively explained as due to the excitation of the heavier  $\Delta$  such as  $\Delta(1650)$  or  $\Delta(1670)$ , the excitation of the  $N^*$  being considerably inhibited by isospin coupling considerations. However the OPE model leads to an energy shift of  $150 \text{ MeV}$  too high. A double  $\Delta(1232)$  excitation seems to correspond to the right energy position in this model.

In conclusion, the two structures appearing in both excitation functions of the  $\text{pd} \rightarrow t\pi$  and  $p\tau \rightarrow \tau p$  for  $\theta_\pi$  and  $\theta_p = 180^\circ$  at the same laboratory kinetic energies of the incident protons are strong indications of the OPE model dominance. A more sophisticated calculation has to be done to relate the  $p\tau \rightarrow \tau p$ ,  $\text{pd} \rightarrow t\pi$  and  $\pi d \rightarrow d\pi$  reaction; in particular to perform correctly the integration over  $q$  in the triangle diagram. The deuteron pick-up term and the rescattering terms have to be taken into account (taking care of the ambiguities arising from double counting).

The first structure is associated with the  $\Delta(1232)$  propagation in  $^2\text{H}$  and  $^3\text{He}$  nuclei, the second one could be explained in the OPE model with a double  $\Delta(1232)$  propagation in these nuclei.

The authors are indebted to S. Buhler and J. Mommejat for the cryogenic  $^3\text{He}$  target and to P. Guillouet and G. Simonneau for their technical support.

#### References

- [1] R. Frascaria et al., Phys. Lett. 66B (1977) 329.
- [2] J. Banaigs et al., to be published; Proc. 9th ICOHEPANS (Versailles, France, July 1981).

- [3] K.R. Chapman et al., Nucl. Phys. 57 (1964) 499.
- [4] J. Franz et al., Phys. Lett. 93B (1980) 384.
- [5] J. Banaigs et al., Phys. Lett. 54B (1973) 394.
- [6] G.W. Barry, Phys. Rev. D7 (1973) 1441.
- [7] R. Frascaria, 9th Intern. Conf. on the Few body problem, Vol. II (Eugene, OR, USA, 1980).
- [8] J.L. Ballot and M. Fabre De La Ripelle, 7th Intern. Conf. on the Few body problem (Delhi, India, 1976); IPNO/TH 8018, Orsay 91406, France.
- [9] R.J. Holt et al., Phys. Rev. Lett. 43 (1979) 1229; R. Frascaria et al., Phys. Lett. 91B (1980) 345; L.S. Schroeder et al., Phys. Rev. Lett. 27 (1971) 1813.
- [10] G.W. Barry, Ann. Phys. (NY) 73 (1972) 482.
- [11] J.C. Anjos et al., Nucl. Phys. A356 (1981) 383.
- [12] B.D. Keister and L.S. Kisslinger, Nucl. Phys. A326 (1979) 445.